Journal of Solid State Electrochemistry (2022) 26:729–738
https://doi.org/10.1007/s10008-021-05108-4

ORIGINAL PAPER

The mechanical hybrid of V_2O_5 microspheres/graphene as an excellent cathode for lithium-ion batteries

Angkang Chen[1] · Chonggui Li[1] · Chaomin Zhang[1] · Wenyao Li[1] · Qi Yang[1]

Received: 14 September 2021 / Revised: 16 November 2021 / Accepted: 16 December 2021 / Published online: 22 January 2022

Abstract

Currently, lithium-ion batteries are widely used in many areas, but they are still limited by the lower cycle stability and energy density. The development of low-cost, environmentally friendly, high-performance methods for the synthesis of graphene-based cathode materials is critical for lithium-ion batteries. Here, V_2O_5 microspheres are synthesized by hydrothermal method. V_2O_5/graphene composite was constructed by wet ball milling. The nanometer-sized V_2O_5 microspheres were well embedded and evenly dispersed into the flexible graphene sheets. Microsphere structure of V_2O_5 reduces the ion transport distance, while the presence of the graphene component enhances the conduction of electrons in V_2O_5@G composites by partially exposing them to the surface of the composites. This study suggests that metal oxide electrodes in integration with graphene can address the poor cycling issues of electrode materials that suffer from low electronic and ionic conductivities. In LIBs, the V_2O_5@G cathode exhibits a discharge capacity of 313.65 mAh g^{-1} at 150 mA g^{-1} (1/2 C) with high specific capacity, and more than 150 mAh g^{-1} at 3A g^{-1} (10 C). After 500 cycles at 150 mA g^{-1}, excellent cycling stability is still maintained. A practical strategy for the development of vanadium-based cathode materials with great promising potential in the field of lithium-based energy storage is provided by this work.

Keywords V_2O_5 · Graphene · Cathode materials · Lithium-ion batteries

Introduction

Today, the growth of energy storage is extremely crucial to the development of sustainable energy solutions and electric vehicles. Recognized as one of the most promising energy storage technologies, lithium-ion batteries have been widely used in portable electronic devices and transportation [1]. In lithium-ion batteries (LIBs), cathode materials play an indispensability role over the energy density and hence extensive research efforts have been focused on the cathode counterparts to exceed the current limitations [2, 3]. Various researchers have established that the rechargeable lithium or lithium-ion battery's storage capacity depends primarily on the cathode material [4, 5]. V_2O_5 is becoming a potential cathode material for high-density Li-ion batteries due to its stable orthogonal crystal layer structure, high theoretical capacity, and multi-electron redox properties [5, 6]. As a prototypical intercalation complex with a crystalline lamellar architecture, it can serve as a suitable host for convertible insertion and extraction of Li+. It can also reach a large theoretical capacity of 294 mAh g^{-1} in the 2.0–4.0 V range, which is comparable to Li/Li^+ [7, 8]. They are higher than those common cathode materials such as $LiCoO_2$ (274mAh g^{-1}), $LiMn_2O_4$ (148 mAh g^{-1}), and $LiFePO_4$ (170 mAh g^{-1}) [9, 10]. However, its low diffusion coefficient (10^{-12} to $10^{-13}cm^2/s$) and conductivity (10^{-2} to $10^{-3}S{\cdot}cm^{-1}$) hinder its large-scale development [11, 12]. So, the practical applications of V_2O_5 electrodes as a cathode in LIBs have been limited to critical issues such as low electrical conduction, slow lithium-ion diffusion, and irreversible phase transitions upon a deep discharge [13]. One of the most effective strategies is to change the structure size of V_2O_5 and combine it with carbon [14–16]. Microspheres effectively improve their electrochemical properties because of the enhanced dynamics of lithium-ion diffusion and electron transport [17–20]. However, the electrochemical performance (both cycling and velocity performance) of V_2O_5 spherical structure is still restricted by its moderate electrical properties, vanadium dissolution, and particle concentration [21].

✉ Chonggui Li
chongguili@sues.edu.cn

[1] School of Materials Engineering, Shanghai University of Engineering Science, Shanghai 201620, China

Graphene is a kind of macromolecular carbon atomic sheet with a honeycomb structure. Due to its high conductivity (10^3–10^4 $S \cdot m^{-1}$), large surface area (about 2630 $m^2 \cdot g^{-1}$) [22, 23], unique graphitization plane structure, and low manufacturing cost, graphene opens a new window for the use of monolayer carbon materials as conductive carriers [24–26]. Its high surface area and outstanding mechanical properties can greatly improve the performance of electrode materials [27, 28]. Over the past few years, a large number of studies have explored the preparation of graphene-based functional substances, such as Co_3O_4/graphene [29], TiO_2/grapheme [30], Fe_3O_4/graphene [31], and Sn/graphene [32]. As for the preparation of graphene-based electrode materials for lithium batteries, there are also some reports, such as graphene-modified $LiFePO_4$ cathode material, which provides 70 mAh g^{-1} capacity at 60 C discharge rate [33]. However, it has a common problem in the preparation of V_2O_5-based electrodes (V_2O_5 and its corresponding hybrid electrodes of V_2O_5/C, V_2O_5/CNTs, and V_2O_5/graphene). It is clear that most of the production methods are quite different from existing industrial processes and they are difficult to mass produce.

In this work, V_2O_5 microspheres are first synthesized by hydrothermal treatment and then compounded with graphene by wet ball-milling method [34]. Here, this composite material was abbreviated as V_2O_5@G [7, 35, 36]. And it provides a way of industrial mass production. By reviewing the literature, mechanical compounding of vanadium pentoxide microspheres and graphene has not been explored, as the structure of microsphere V_2O_5 greatly reduces the diffusion distance of lithium ions and improves its performance [37]. The materials of V_2O_5 benefit from the high electronic conductivity of graphene and exhibit excellent electrochemical performance for lithium-ion. The electrochemical properties of the composite cathode were investigated by various electrochemical testing techniques based on the morphology and structure of the V_2O_5 microspheres/graphene composite.

Experimental

Preparation of V_2O_5@G

A total of 1.2 g vanadium pentoxide was dissolved in 40 mL deionized water, then 2.4 g oxalic acid was added to the previous solution, stirring the mixture until the solution became blue. Then, the prepared solution was transferred to a hydrothermal reactor and reacted at 210 °C for 24 h. After cooling, the precipitate was collected by centrifugation, washed vigorously with ethyl acetate, and dried at 80 °C for 12 h. After annealing at 350 °C for 2 h with a heating rate of 1 °C·min^{-1}, the products were transformed into V_2O_5 microspheres. (In this paper, V_2O_5 was produced by heating NH_4VO_3 (99%) in air at 350 °C for 2 h.)

Here, we collect 0.2 g V_2O_5 microspheres and 0.02 g graphene powder (physical graphene, purchased by YunShan Technology). Then, two materials were loaded separately inside a stainless steel milling container together with four hardened steel balls (diameter of 25.4 mm) along with a suitable amount of acetone as solvent. Both mixtures were milled in a rolling ball mill at a rotation speed of 120 r/min for 25 h at room temperature under an argon atmosphere of 100 kPa. Finally, the powder was placed in a vacuum drying oven at 80 °C for 10 h to obtain V_2O_5 and graphene composites. The overall preparation process is shown in Fig. 1.

Structural characterization

The crystal structure is determined by X-ray diffraction (XRD, RigakuD/max2500XRD, and copper Kα radiation, $\lambda = 1.54178$ Å). The form and architecture of the components were identified through scanning electron microscopy (SEM, Hitachi S-3400 N). Thermogravimetric analysis (TGA) was performed via a Q50 Thermogravimetric Analyzer in air to determine the actual amount of carbon in the hybrid samples. Transmission electron microscopy (TEM) investigations were performed using a JEOL JEM 2100F instrument operated at 200 kV. For comparison, the specific surface area (determined by Brunauer-EmmettTeller (BET) method) and nitrogen adsorption isotherms of V_2O_5 and V_2O_5@G samples were measured.

Electrochemical determination

The electrochemical properties of V_2O_5 and graphene composites were studied in a two-electrode coin cell (CR2032). The composite material with a weight ratio of 80:10:10, mixing acetylene black and polyvinylidene fluoride binder together, and then dispersed in N-methyl-2 -pyrrolidone (NMP) solution to prepare the slurry. The slurry was coated on aluminum foil and dried overnight in a vacuum oven at 80 °C before the coin battery assembly. In this experiment, the slurry thickness on top of the aluminum foil was 60 μm and was applied by a squeegee. The semi-battery pack was installed in a glove box with ultra-high purity argon. Polypropylene films were used as separators and 1.0 M $LiPF_6$ dissolved in ethylene carbonate/dimethyl carbonate (EC/DMC) = 1:1 (volume ratio) as cyanide. Lithium metal was used as counter electrode and reference electrode. The constant current charge–discharge characteristics of the battery were obtained on the terrestrial battery tester (terrestrial CT 2001 A, Wuhan, China) in the voltage range of 2.0–4.0 V (relative to cyclic ambient voltammetry (CV); 2.0–4.0 V, 0.1 ms^{-1}) and were measured by CHI 660E electrochemical workstation (at room Li/Li^+). The mass load of cathode material is about 1.5 mg/cm^2, and the specific capacity is only according to the mass of inactive ingredients.

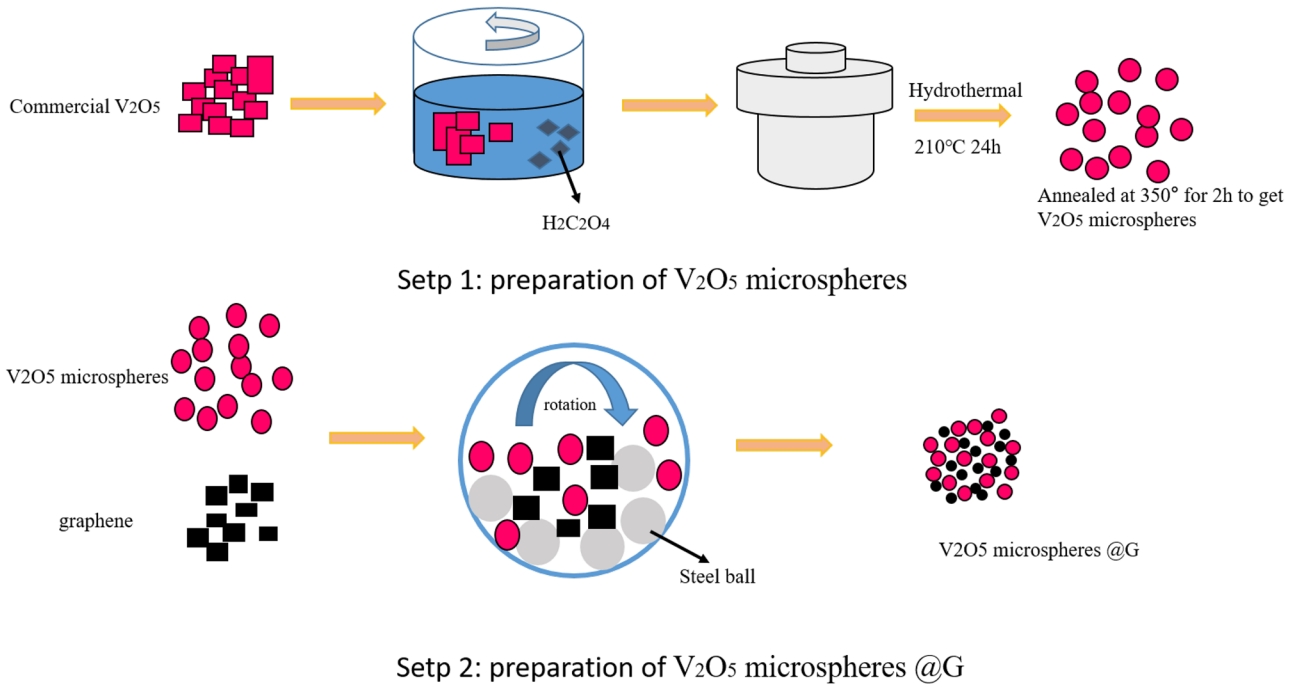

Fig. 1 Schematic diagram of material preparation

Results and discussion

Morphology and structure

XRD characteristics were measured to identify the compositions of the samples V_2O_5 and V_2O_5@G. Figure 2 shows the depicted XRD pattern, where the corresponding diffraction peaks in the main plane (200), (001), and (301) of the two samples are assigned as characteristic diffraction peaks of the orthorhombic phase V_2O_5, conforms to JCPDS Standard Card No. 41–1426 and belongs to the space group of Pmmn (59) (a = 11.516 Å, b = 3.566 Å, c = 4.373 Å). It indicates that the main component of the two samples is V_2O_5 [33, 34]. In addition, in Fig. 1, the weak and wide diffraction peaks near 24° overlap partially with the (110) plane of V_2O_5 and cannot be clearly identified characteristic diffraction peaks of graphene. In addition, V_2O_5@G composites showed a similar XRD pattern to pure V_2O_5, and no peaks of carbon species were observed in the composite. It might be due to the low mass content and relatively low diffraction intensity of graphene [38].

To further insight into the morphology of composites, the sample V_2O_5 was tested by SEM. SEM images of V_2O_5 microsphere materials and graphene used in the experiment are shown in Fig. 3. Here, V_2O_5 and oxalic acid are used as raw materials. V_2O_5 microspheres were prepared in one step by a hydrothermal method. In this study, VO_2 microspheres were generated by solvothermal reaction at 210 °C for 4 h in the presence of ethylene glycol. The results showed that the structure of VO_2 microspheres was improved after annealing at 350 ℃ for 2 h. Two-dimensional graphene exfoliated by mechanical method is shown in Fig. 3c, d. XRD pattern indicated that VO_2 was completely converted to V_2O_5. The XRD peaks of the synthesized products are well indexed and assigned to the orthogonal structure of the V_2O_5 phase with the Pmmn (56) space group. Observation by scanning electron microscopy shows that the average diameter of the

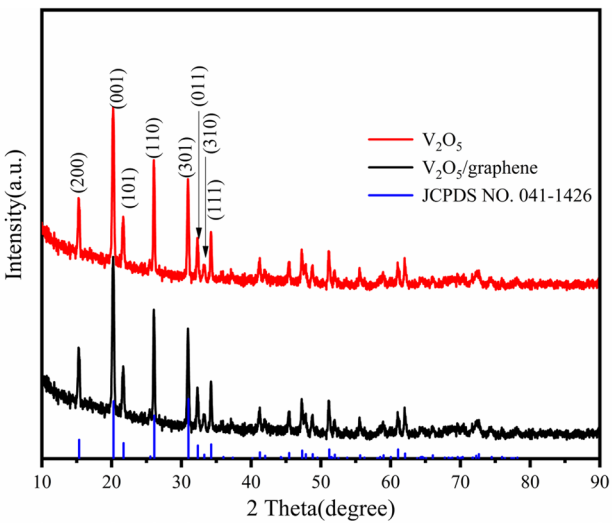

Fig. 2 XRD pattern of V_2O_5 and V_2O_5@G composites

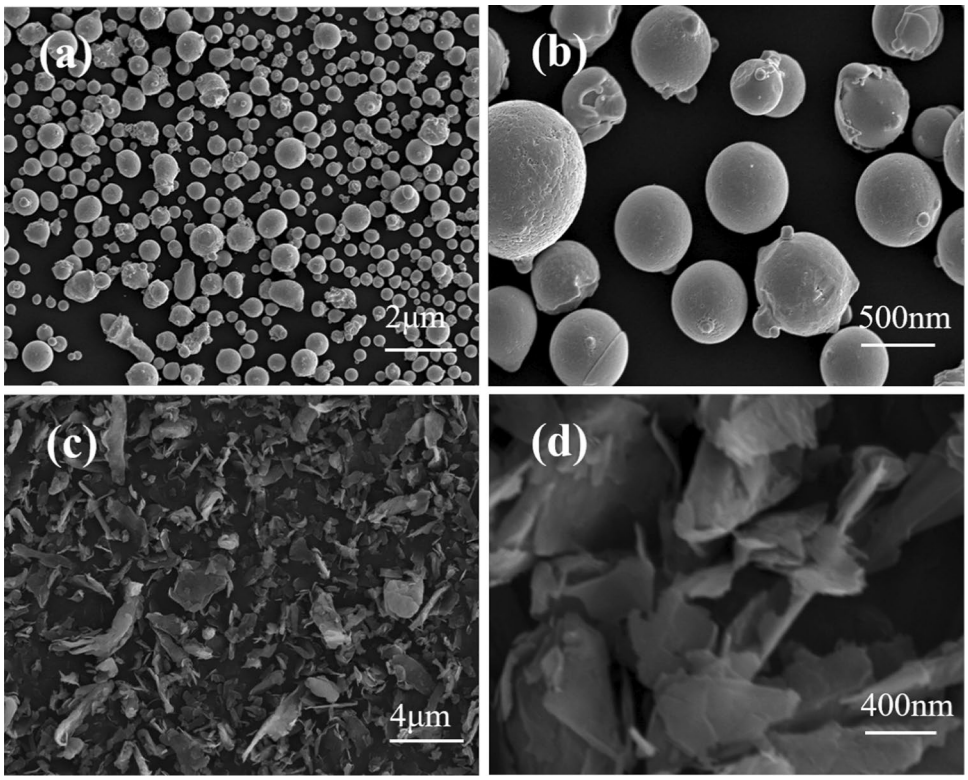

Fig. 3 FESEM (**a**, **b**) images of the V_2O_5 microspheres, and (**c**, **d**) images of the graphene

solid V_2O_5 microspheres is 1 μm and has a uniform spherical shape.

In purpose of visualizing the element distribution in the composites, the V_2O_5@G composites were characterized by scanning electron microscopy and energy spectrometry, as shown in Fig. 4. The composite structure of the sample vanadium pentoxide and graphene also presents a spherical structure. By comparing the morphology of the uncomposited vanadium pentoxide, it can be found that the composite graphene has little effect on the morphology of the sample, and it still shows a uniform spherical structure.

As shown in Fig. 4, the images of elemental distribution of the compound show that oxygen, vanadium, and carbon are uniformly spread in the composite of vanadium pentoxide and graphene. Figure 4c illustrates the distribution of carbon elements, with conductive adhesive as the test substrate, and the sample shows a dark covered area, indicating that the quantity of carbon elements in the V_2O_5@G composite is very small.

To get more insight into the morphological aspects of pristine V_2O_5 and graphene composites, HRTEM was employed (Fig. 5). Figure 5a illustrates the HRTEM images of V_2O_5 with lattice fringe d-spacing of 0.33 nm corresponding to (200) plane which further confirms the high crystallinity of V_2O_5. Dense agglomeration of V_2O_5 nanoparticles was observed in the TEM samples. The V_2O_5 nanoparticles/aggregates are dispersed on the surface of graphene sheets and wrapped by a small amount of graphene. The usually wrinkled graphene sheets form a network and cover the highly dispersed V_2O_5 nanoparticles/aggregates, thus significantly increasing the electrical conductivity and stabilizing the cathode structure of the hybrid system.

The amount of graphene present in the V_2O_5@G composite was estimated by thermogravimetric analysis (Fig. 6). The weight loss observed in the temperature range of 400–500 °C was found to be 8.5%, which can be attributed to the decomposition of graphene present in the composite. Based on the TG results, the ratio of V_2O_5 to graphene was estimated to be 91.5:8.5 in this composite.

Electrochemical properties of products

In order to study the electrochemical performance of V_2O_5@G as cathode material for lithium-ion battery, the cyclic performance and rate performance were tested by constant current charge–discharge, the electrode process was studied by cyclic voltammetry, and the mechanism was studied by AC impedance spectroscopy.

In purpose of investigating the effect of graphene synthesis on the cyclic stability of the composites, we examine the detailed electrochemical properties of the LIBs with V_2O_5@G as the cathode active materials. Figure 7a shows the specific discharge capacity of the sample V_2O_5@G at a rate of current up to 150 mA g^{-1}. It is observed that the specific discharge capacity of the sample is 313.65 mAh g^{-1} at a voltage window of 2.0–4.0 V for the second turn. After

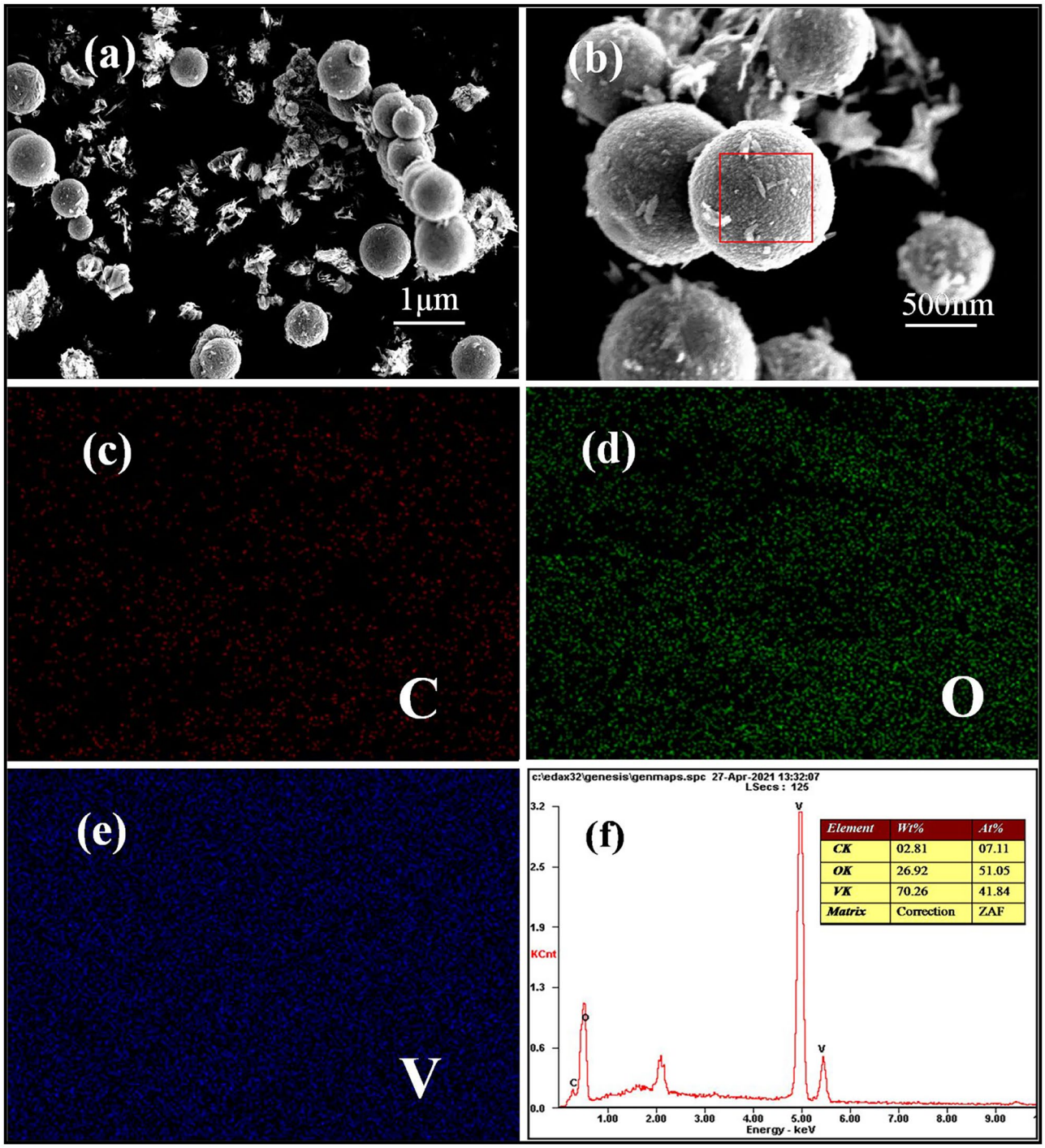

Fig. 4 V_2O_5@G composites. (**a**, **b**) SEM image. The spatial distribution of elements maps for (**c**) C, (**d**) O, (**e**) V, and (**f**) EDS spectra

the 50th charge/discharge cycle, the composites provided a relatively high specific discharge capacity of 300.5 mAh g^{-1} and maintained a capacity retention of 96% (compared to the specific discharge capacity of the second cycle.) The representative specific discharge capacity of the V_2O_5 powder sample was 168.2 mA g^{-1}, while the capacity retention was 53.7%. Thus, the V_2O_5@G composite exhibited significantly improved cycling stability, 38% higher than the unblended sample V_2O_5. The decrease of V_2O_5 size in the composite sample, on the one hand, generates a larger specific surface area, increasing the contact area between the electrolyte and the electrode, which is conducive to the achievement of good cycling stability. On the other hand, graphene with better conductivity is sandwiched between the vanadium pentoxide

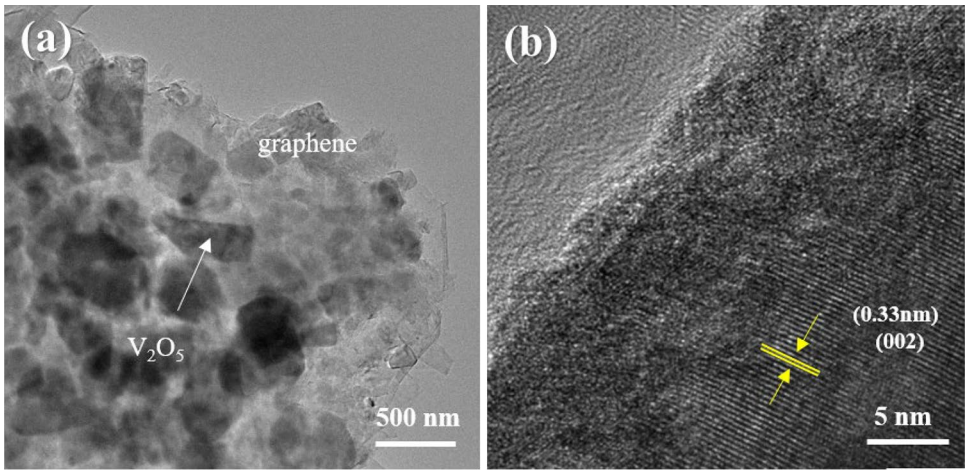

Fig. 5 Structural analysis of the V_2O_5@G. (**a**) Low-magnification TEM image. (**b**) High magnification TEM images (overlaid scheme; structural model for monoclinic V_2O_5 along the (002) plane)

microspheres, which accelerates the effective transfer of ions and electrons and thus achieves high volume preservation. Cycle performance of V_2O_5@G and V_2O_5 is revealed in Fig. 7b. The V_2O_5@G electrode could maintain a high reversible specific capacity of 313.65 mAh g^{-1} even after 200 cycles at a current density of 0.5 C, corresponding to the capacity retention of 68% (calculated from the first discharge capacity). In contrast, the individual V_2O_5 only delivered a capacity of 89 mAh g^{-1} (33% capacity retention). Figure 7c shows the charge/discharge curves of the V_2O_5@G composite for different rates. The working potential is essentially constant and the discharge/charge plateau is still observed even at higher rates. The voltage gap is much smaller than that and the capacity is much larger than that of the V_2O_5 powder. The results indicate that the assembled V_2O_5@G composites have a lower polarization, which may be attributed to the special structure of the V_2O_5 spheres that greatly reduces the inter-ion transport distance. Figure 7d shows the rate performance of the V_2O_5@G composite electrode. Reversible capacities of approximately 313, 255, 187, 155, and 281 mAh g^{-1} are provided at high discharge rates of 0.5 C, 1 C, 5 C,10 C, and 0.5 C, respectively, while the bare V_2O_5 electrodes inspected under the same conditions only show 210, 175, 130, 75, and 153 mAh g^{-1}. Everyone can see that the specific capacity of V_2O_5@G is higher than V_2O_5 powder under different current densities. When the discharge/charge rate is reset to 0.5 C, the composite material can recover to a high discharge capacity of 281 mAh g^{-1}. And the coulombic efficiency of the composite material is close to 100% throughout the discharge/charge process. This result indicates that V_2O_5@G has better rate performance because of the good electrical conductivity of V_2O_5 and graphene composites, and the spherical V_2O_5 increases the specific surface area of the active material, which leads to excellent performance.

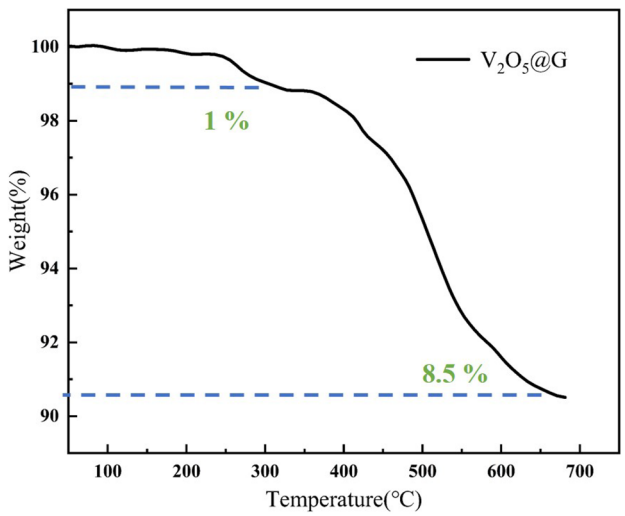

Fig. 6 TG curve of V_2O_5@G

BET measurement was used to estimate the surface area and pore structure of V_2O_5@G microspheres and pure V_2O_5 powders, as shown in Fig. 6. Due to the unique sphere structure, the BET surface area of V_2O_5@G microspheres arrived at 78.48 m^2/g, which was almost five times higher than that of pure V_2O_5 (16.32 m^2/g). The high surface area of V_2O_5@G microspheres could provide more Li-ions and increase the contact area between electrodes and electrolytes. In Fig. 8a, the absorption quantity of N_2 for V_2O_5@G microspheres increased significantly with increased pressure, indicating the existence of many pores. Moreover, the distribution of pore size was also measured using the nitrogen adsorption method (Fig. 8b). The pores in V_2O_5@G microspheres consisted of mesopores and macropores, and the pore size was concentrated at 120 nm, which indicated that many macropores were existing in the V_2O_5 microspheres. The large specific surface area and high pore volume of electrode materials could also improve the contact area between electrodes and

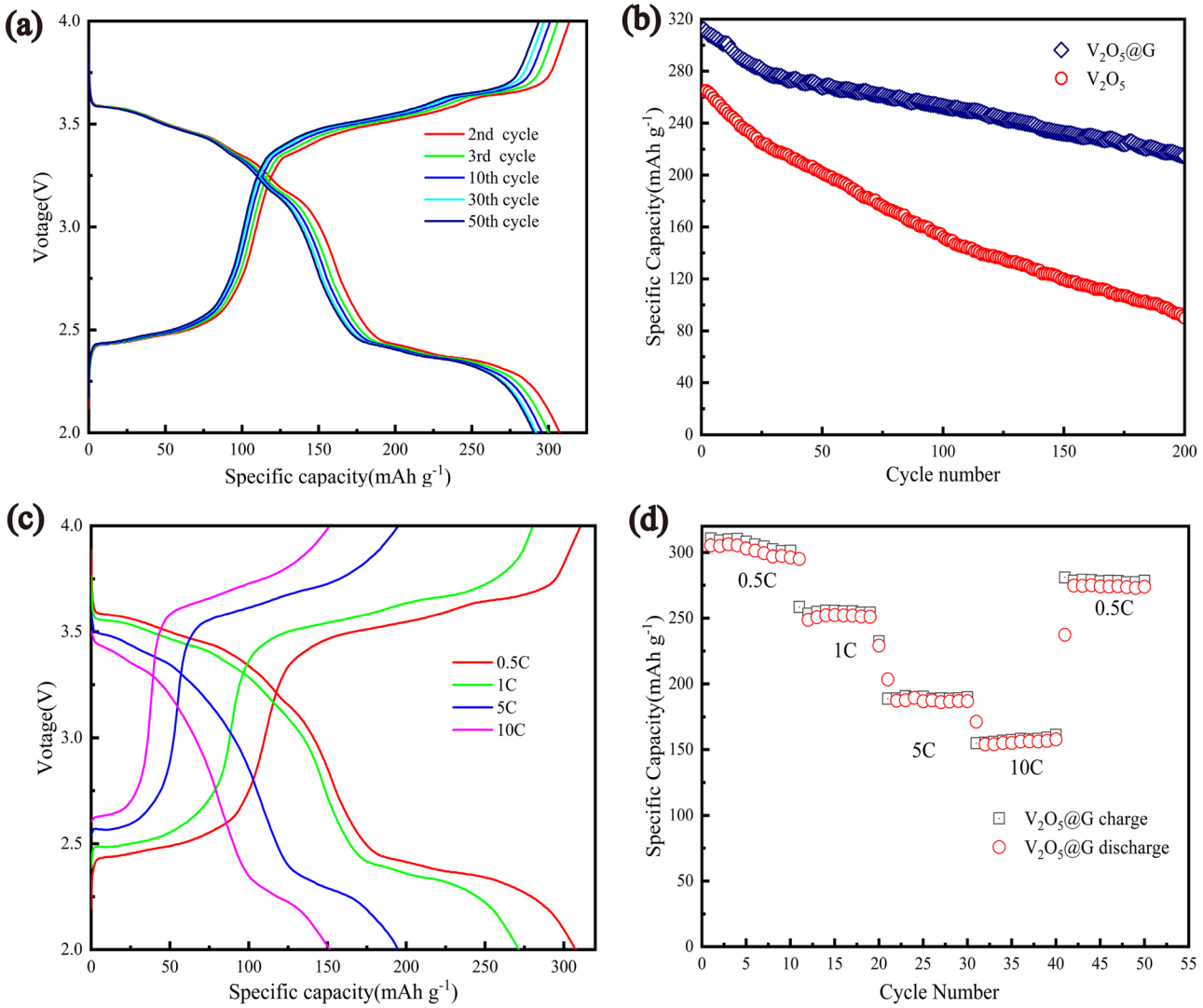

Fig. 7 (**a**) Discharge/charge curves for selected cycles of V_2O_5@G at a current density of 150 mA g^{-1}. (**b**) Cycling performances of V_2O_5@G and V_2O_5. (**c**) Cycle curves of V_2O_5@G under different current densities. (**d**) Charge/discharge capacities of V_2O_5@G at different current rates

electrolytes, and have a great potential in improving the storage capacity of LIBs.

To investigate the oxidation–reduction reaction and the phase transition of electropolymer of electrode material in electrochemical reaction, the cyclic voltammetric curves of V_2O_5@G composite were measured. The voltage range was 2.0–4.0 V and the scanning rate was 0.1 mV·s^{-1}. For clarity, only the second and third cycles are shown. In Fig. 9, the CV curves for both pristine and composite electrodes show three distinct reduction peaks at 3.4, 3.2, and 2.3 V

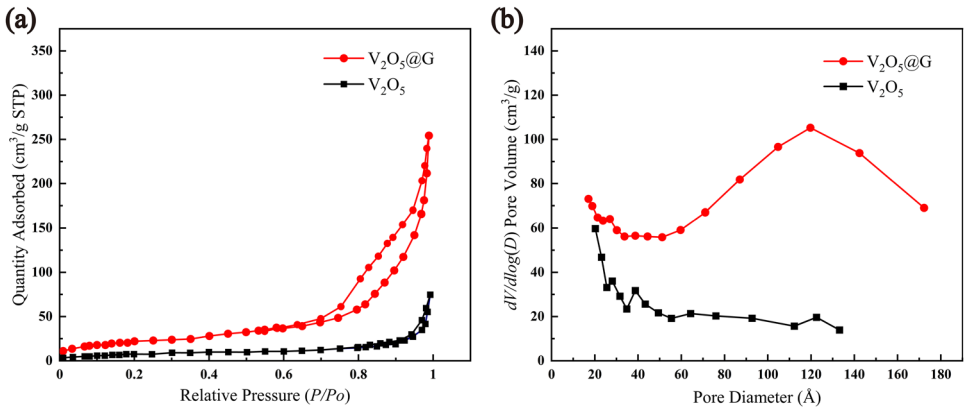

Fig. 8 N_2 adsorption under different pressures (**a**) and pore structure (**b**) of V_2O_5@G and pure V_2O_5 powders

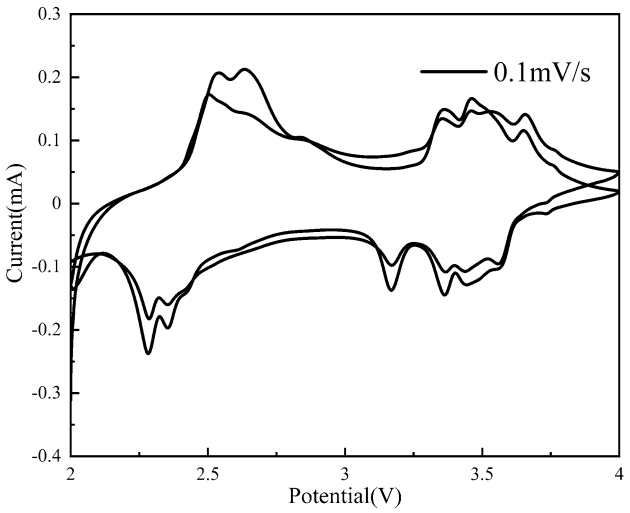

Fig. 9 Cyclic voltammograms of V_2O_5@G at a scan rate of 0.1 mV·s^{-1}

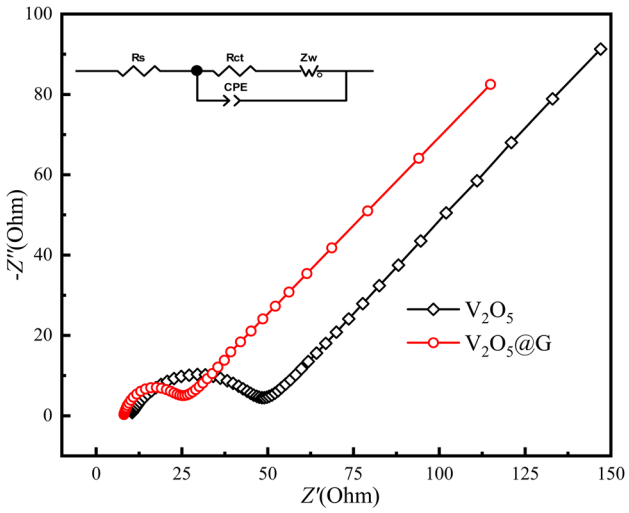

Fig. 10 Comparable Nyquist plots before charge–discharge testing (inset: a simplified equivalent circuit)

(vs. Li/Li$^+$). Referring to the oxidation/reduction process of $V^{3+/5+}$, and the corresponding phase change process was from α-V_2O_5 to ε-$Li_{0.5}V_2O_5$, then to δ-LiV_2O_5, and finally to γ-Li_2VO_5. In the anode scan, the peak appears at 2.6, 3.5, and 3.6 V that indicates a reversible phase transition of V_2O_5. V_2O_5 receives two Li^+ during the discharge process and transforms into disordered $Li_2V_2O_5$. After Li^+ is removed during the charging process, $Li_2V_2O_5$ subsequently restores its original layered V_2O_5 structure. The V_2O_5@G composites exhibit a narrower potential gap and higher core current density between the major redox peaks, which fully explains the faster Li + transport rate between the electrode and electrolyte polarization. Three distinct potential plateaus can also be observed in the charging curve, again corresponding to the three oxidation peaks during the forward scan of the cyclic voltammetric curve, as well as the three lithium ion de-embedding reactions of the formula.

The influence of graphene on the charge conversion process was studied by AC impedance measurement of samples. The results of electrochemical impedance spectra are shown in Fig. 10, where a simplification of the EIS fitted with an equivalent circuit is inserted. *Rct* denotes the charge transferred immunity, which mainly mirrors the electric and ionic conductivity, *Rs* denotes the ohms impedance, *Zw* denotes

Table 1 Electrochemical properties of different composites of vanadium pentoxide

Electrode material	Voltage window (V)	Current density	Specific capacity (mAh g^{-1})
V_2O_5@WMWCNT [39]	2–4	0.1 C	265
		1 C	180
		5 C	116
V_2O_5@G Nanoribbon [40]	2–4	0.1 C	278
		2 C	165
V_2O_5 nanoribbon/graphene [41]	2–4	1 C	275
		10 C	225
V_2O_5 nanoribbon/RGO [42]	2–4	2 C	125
		5 C	97
Sandwich-like V_2O_5 Nanosheets/G [43]	2–4	0.5 C	275
		1 C	250
		2 C	230
V_2O_5/Mesoporous carbon [44]	2–4	100 mAh g^{-1}	291
		250 mAh g^{-1}	265
		500 mAh g^{-1}	247
This work	2–4	0.5 C	313
		1 C	255
		5 C	187
		10 C	155

the Warburg resistance, which captures the diffusion of Li + in the electrode material, and CPE denotes the two-layer capacitance. The immunity test of a triple-electrode solution contains a one-half circle in the high frequency domain and a diagonal in the low spectrum, which are matched to the charge shift resistance (*Rct*) and the ion diffusion impedance, respectively. The fitting results of the two samples show that the charge transfer resistance of V_2O_5 and V_2O_5@G are 73.6Ω and 27.9Ω, respectively. Obviously, the V_2O_5@G composite exhibits a small charge transfer resistance, indicating that electrons and ions transfer faster at the interface between the electrode V_2O_5@G and the electrolyte. This is chiefly attributable to the fact that the addition of graphene boosts the electrical properties of the composites which facilitates the transport of both electrons and ions across a liquid–solid boundary. Table 1 lists the performance of the V_2O_5-based electrodes compared with previously reported electrodes.

As shown in Table 1, the ball-milled composite V_2O_5@G has a larger capacity and better rate capability than many other V_2O_5-based electrodes. The excellent velocity and outstanding cycling stability can be attributed to the synergistic performance effects between the vanadium pentoxide and graphene substrates, including the following two points. (1) Graphene ensures good electronic conductivity of the electrode material; (2) the spherical structure of V_2O_5 can greatly enlarge the contact area between the electrolyte and the polarized electrode material.

Conclusions

In brief, V_2O_5 microspheres were produced by a straightforward hydrothermal method. V_2O_5@G composites were formed by ball milling with graphene powder and V_2O_5 under vacuum gas. The results show that after 200 cycles of 150 mAh g^{-1}, the capacitance retention of the V_2O_5@G composite is 78.5%, which is 40% more than that of the non-compounded V_2O_5 materials. V_2O_5@G as cathode materials have a stable capacity after 500 cycles. They also offer good circulation stability and capacity retention of more than 150mAh g^{-1} at high current densities of 10C. This is because the microspherical V_2O_5 shortens the ion transport distance and the high conductivity of graphene effectively improves the conductivity and cycling stability of V_2O_5 at high current densities. This simple composite approach provides feasibility for industrial implementation of vanadium oxide cathode materials.

Funding This work was financially supported by the National Natural Science Foundation of China (51402189), and Shanghai Research Project of Science and Technology Innovation Action Program (16030501100).

References

1. Dunn B, Kamath H, Tarascon JM (2011) Electrical energy storage for the grid: a battery of choices. Science 334:928–935
2. Myung ST, Maglia F, Park KJ, Chong SY, Sun YK (2016) Nickel-rich layered cathode materials for automotive lithium-ion batteries: achievements and perspectives. ACS Energy Lett 2:196–223
3. Whittingham MS (2004) Lithium batteries and cathode materials. Chem Rev 35:4271–4301
4. Shi Y, Guo B, Corr SA, Shi Q, Stucky GD (2009) Ordered mesoporous metallic MoO2 materials with highly reversible lithium storage capacity. Nano Lett 9:4215
5. Fergus JW (2010) Recent developments in cathode materials for lithium ion batteries. J Power Sources 195:939–954
6. Rui X, Sim D, Xu C, Liu W, Tan H, Wong K, Hng HH, Lim TM, Yan Q (2012) One-pot synthesis of carbon-coated VO_2(B) nanobelts for high-rate lithium storage. RSC ADVANCES
7. Rong Y, Cao Y, Guo N, Li Y, Jia W, Jia D (2016) A simple method to synthesize V_2O_5 nanostructures with controllable morphology for high performance Li-ion batteries. Electrochim Acta 222:1691–1699
8. Delmas C, Cognac-Auradou H, Cocciantelli JM, Ménétrier M, Doumerc JP (1994) The LixV2O5 system: an overview of the structure modifications induced by the lithium intercalation. Solid State Ionics 69:257–264
9. Han T, Peng Z, Lu W, Xiong F, Pei C, An Q, Mai L (2018) Vanadium-based cathode materials for rechargeable multivalent batteries: challenges and opportunities. Electrochem Energ Rev
10. Wu C, Dai J, Zhang X, Yang J, Qi F, Gao C, Xie Y (2010) Direct confined-space combustion forming monoclinic vanadium dioxides. Angew Chem 49:134–137
11. Cheng J, Gu G, Guan Q, Razal JM, Wang Z, Li X, Wang B (2016) Synthesis of a porous sheet-like V_2O_5–CNT nanocomposite using an ice-templating 'bricks-and-mortar' assembly approach as a high-capacity, long cyclelife cathode material for lithium-ion batteries. J Mater Chem A 4
12. Li Y, Yao J, Uchaker E, Yang J, Huang Y, Zhang M, Cao G (2013) Leaf-like V_2O_5 nanosheets fabricated by a facile green approach as high energy cathode material for lithium-ion batteries. Adv Energy Mater 3:1171–1175
13. Minsu L, Bin Su, Yue T, Xuchuan J, Aibing Yu (2017) Recent advances in nanostructured vanadium oxides and composites for energy conversion. Adv Energy Mater 7:1700885
14. Liu J, Zhou Y, Wang J, Pan Y, Xue D (2011) Template-free solvothermal synthesis of yolk-shell V_2O_5 microspheres as cathode materials for Li-ion batteries. Chem Commun 47:10380–10382
15. Wang ZL, Xu D, Wang LM, Zhang XB (2012) Facile and low-cost synthesis of large-area pure V2O5 nanosheets for high-capacity and high-rate lithium storage over a wide temperature range. ChemPlusChem
16. Zhou X, Wu G, Gao G, Wang J, Zhang Z (2012) Electrochemical performance improvement of vanadium oxide nanotubes as cathode materials for lithium ion batteries through ferric ion exchange technique. Jphyschemc 116:21685–21692
17. Pan A, Wu HB, Yu L, Lou XW (2013) Template-free synthesis of VO_2 hollow microspheres with various interiors and their conversion into V_2O_5 for lithium-ion batteries. Angewandte Chemie International Edition
18. Yu S, Ng V, Wang F, Xiao Z, Li C, Ling BK, Que W, Zhou K (2018) Synthesis and application of iron-based nanomaterials as anodes of lithium-ion batteries and supercapacitors. J Mater Chem A 6
19. Rui X, Zhao X, Lu Z, Tan H, Sim D, Hng HH, Yazami R, Lim TM, Yan Q (2013) Olivine-type nanosheets for lithium ion battery cathodes. ACS Nano 7:5637–5646

20. Sun YK, Chen Z, Noh HJ, Lee DJ, Jung HG, Yang R, Wang S, Chong SY, Myung ST, Amine K (2012) Nanostructured high-energy cathode materials for advanced lithium batteries. Nat Mater 11:942–947
21. West K, Zachau-Christiansen B, Jacobsen T, Skaarup S (1993) Vanadium oxide xerogels as electrodes for lithium batteries. Electrochim Acta 38:1215–1220
22. Zhu Y, Murali S, Cai W, Li X, Ji WS, Potts JR, Ruoff RS (2010) ChemInform abstract: graphene and graphene oxide: synthesis, properties, and applications. ChemInform 41
23. Ding C, Zhao Y, Yan D, Zhao Y, Zhou H, Li J, Jin H (2016) An insight into the convenience and efficiency of the freeze-drying route to construct 3D graphene-based hybrids for lithium-ion batteries. Electrochim Acta 221:124–132
24. Sakamoto JS, Dunn B (2002) Vanadium oxide-carbon nanotube composite electrodes for use in secondary lithium batteries. ChemInform 33:A26–A30
25. Suzuki S, Hibino M, Miyayama M (2003) High rate lithium intercalation properties of V_2O_5/carbon/ceramic-filler composites. J Power Sources 124:513–517
26. Zhu Y, Murali S, Stoller M, Ganesh KJ, Ruoff RS (2011) Carbon-based supercapacitors produced by activation of graphene. Science 332:1537–1541
27. Chengzhi, Wang, Yongjie, Zhao, Ximei, Zhai, Xiuchen, Zhao, Jingbo (2018) Confining ferric oxides in porous carbon for efficient lithium storage. Electrochimica Acta
28. Cd A, Yz A, Dong YB, Ds A, Yz C, Hz C, Jl A, Hj A (2017) Construction of Zn_2 GeO_4/graphene nanostructures with dually-protected functional nanoframes for enhanced lithium-storage performances. Electrochim Acta 251:129–136
29. Liang Y, Li Y, Wang H, Zhou J, Wang J, Regier T, Dai H (2011) Co_3O_4 nanocrystals on graphene as a synergistic catalyst for oxygen reduction reaction. Nat Mater 10:780–786
30. Kim AY, Kim J, Kim MY, Ha SW, Ngyen Thi Thuy T, Kang M (2012) Photovoltaic efficiencies on dye-sensitized solar cells assembled with graphene-linked TiO_2 anode films. Bull Korean Chem Soc 33:3355–3360
31. Wang H, Xu Z, Yi H, Wei H, Guo Z, Wang X (2014) One-step preparation of single-crystalline Fe_2O_3 particles/graphene composite hydrogels as high performance anode materials for supercapacitors. Nano Energy 7:86–96
32. Qu B, Ma C, Ji G, Xu C, Xu J, Meng YS, Wang T, Lee JY (2014) Layered SnS2-reduced graphene oxide composite - a high-capacity, high-rate, and long-cycle life sodium-ion battery anode material. Adv Mater 26:3854–3859
33. Zhou X, Wang F, Zhu Y, Liu Z (2011) Graphene modified $LiFePO_4$ cathode materials for high power lithium ion batteries. J Mater Chem 21:3353–3358
34. Shan Y, Xu L, Hu Y, Jiang H, Li C (2019) Internal-diffusion controlled synthesis of V_2O_5 hollow microspheres for superior lithium-ion full batteries. Chem Eng Sci
35. Chen J, Li W, Jian J, Chao W, Liu Y (2016) Facile and creative design of hierarchical vanadium oxides@graphene nanosheet patterns. RSC Adv 6:13323–13327
36. Hy A, Sw A, Yh A, Gh B, Le Q, Ipp B, Hao JA (2020) Lithium-conductive LiNbO 3 coated high-voltage LiNi 0.5 Co 0.2 Mn 0.3 O 2 cathode with enhanced rate and cyclability. Green Energy Environ
37. Su DW, Dou SX, Wang GX (2014) Hierarchical orthorhombic V_2O_5 hollow nanospheres as high performance cathode materials for sodium-ion batteries. J Mater Chem A 2:11185
38. Guo Y, Huang Y, Jia D, Wang X, Sharma N, Guo Z, Tang X (2014) Preparation and electrochemical properties of high-capacity $LiFePO_4$-$Li_3V_2(PO_4)_3$/C composite for lithium-ion batteries. J Power Sources 246:912–917
39. Partheeban T, Kesavan T, Vivekanantha M, Sasidharan M (2019) One-pot solvothermal synthesis of V_2O_5/MWCNT composite cathode for Li ion batteries. Appl Surf Sci 493
40. Yang Y, Li L, Fei H, Peng Z, Tour JM (2014) Graphene nanoribbon/ V_2O_5 cathodes in lithium-ion batteries. ACS Appl Mater Interfaces 6:9590–9594
41. Jing ZA, Jh A, Jl A, Tian XA, Cp A, Yl A, Pl A, Rza C, Jie MB (2019) Self-assembly of single layer V 2 O 5 nanoribbon/graphene heterostructures as ultrahigh-performance cathode materials for lithium-ion batteries. Carbon 154:24–32
42. Chen D, Quan H, Luo S, Luo X, Jiang H (2014) Reduced graphene oxide enwrapped vanadium pentoxide nanorods as cathode materials for lithium-ion batteries. Physica E 56:231–237
43. Wu L, Zhang Y, Fan L, Zhang Q, Wang P, Tian D, Zhang N, Sun K (2018) Fabrication sandwich-like V_2O_5 nanosheets anchor in graphene towards high energy lithium cathode materials. Energy Technol
44. Ihsan M, Meng Q, Li L, Li D, Wang H, Seng KH, Chen Z, Kennedy SJ, Guo Z, Liu H-K (2015) V_2O_5/mesoporous carbon composite as a cathode material for lithium-ion batteries. Electrochim Acta 173:172–177